DOI: 10.1002/chem.201104061

[2]Catenanes Built Around Octahedral Transition-Metal Complexes that Contain Two Intertwined Endocyclic but Non-sterically Hindering Tridentate Ligands

Jean-François Ayme,[a] Jacques Lux,[a] Jean-Pierre Sauvage,*[a, b] and Angélique Sour*[a]

Abstract: Sterically hindering bidentate chelates, such as 2,9-diphenyl-1,10-phenanthroline, form entwined complexes with copper(I) and other tetrahedrally coordinated transition-metal centres. To prepare octahedral complexes containing two entwined tridentate ligands and thus apply a strategy similar to that used for making catenanes with tetrahedral metal centres, the use of the classical terpy ligand (terpy = 2,2′:6′,2″-terpyridine) appears to be attractive. In fact, 6,6″-diphenyl-2,2′:6′,2″-terpyridine (dp-terpy) is not appropriate due to strong "pinching" of the organic backbone by coordination to the metal and thus stable entwined complexes with this ligand cannot be obtained. Herein, we report the synthesis and coordination properties of a new family of tridentate ligands, the main features of which are their endocyclic nature and non-sterically hindering character. The coordinating fragment consists of two 8′-phenylisoquinolin-3′-yl groups attached at the 2 and 6 positions of a pyridine nucleus. Octahedral complexes containing two such entangled ligands around an octahedral metal centre, such as Fe^{II}, Ru^{II} or Co^{III}, are highly stable, with no steric congestion around the metal. By using functionalised ligands bearing terminal olefins, double ring-closing metathesis leads to [2]catenanes in good yield with Fe^{II} or Co^{III} as the templating metal centre. The X-ray crystallography structures of the Fe^{II} precursor and the Fe^{II} catenane are also reported. These show that although significant pinching of the ligand is observed in both Fe^{II} complexes, the system is very open and no steric constraints can be detected.

Keywords: catenanes · entwined ligands · isoquinoline · transition metals · tridentate ligands

Introduction

Transition metals have played and continue to play a very important role in the synthesis of catenanes and rotaxanes.[1–18] The first high-yielding template synthesis, reported long ago,[10] was based on copper(I), which is able to bind two bidentate coordinating fragments so as to generate a two-component entanglement, that is, a precursor to a [2]catenane. Transition metals have been amply used by various groups to prepare a large variety of interlocking-ring compounds.[11–30] More recently, an important extension has been reported, named the "active metal template", which consists of using the metal as both a structural element able to gather and orient the various organic fragments to be incorporated in the catenane backbone and a reagent or even a catalyst for the last step of the synthesis, namely the ring-closing reaction for catenanes or the stopper-fixing step for rotaxanes.[31–38] This last approach paves the way for the synthesis of interlocking compounds by using catalytic amounts of a transition-metal complex instead of stoichiometric quantities. Traditionally, copper(I)—generally considered to be a tetrahedrally coordinated metal centre—has been the metal of choice as the template and even as the "active template", in association with one or two bidentate ligands, although other transition metals (palladium, in particular) have also been utilised.

Octahedral transition-metal complexes have also been used in the traditional approach, when the function of the metal centre is purely structural, most of the time with remarkable success in terms of simplicity and the efficiency of the synthesis.[18,25–30] Particularly interesting work by Leigh and co-workers was reported ten years ago,[19a] which showed that a large variety of octahedral metal centres can indeed be used as very efficient templates when used in conjunction with two entangled tridentate ligands. In recent reports, we described the remarkable properties of a new family of bidentate ligands based on the 8,8′-diphenyl-substituted 3,3′-biisoquinoline fragments (dpbiiq). These fragments are crescent shaped, thereby allowing the incorporation of such ligands in a ring with an endocyclic coordination site, and at the same time they have a very open coordination site. The dpbiiq-type ligands are thus simultaneously endocyclic and non-sterically hindering.[27,39]

We would now like to report that this concept can be extended to tridentate chelating groups incorporating two substituted isoquinoline fragments attached to a central pyridine nucleus. The archetypal tridentate ligand of this type is

[a] J.-F. Ayme, Dr. J. Lux, Dr. J.-P. Sauvage, Dr. A. Sour
Laboratoire de Chimie Organo-Minérale, Institut de Chimie
University de Strasbourg-CNRS/UMR7177
4 rue Blaise Pascal, 67070 Strasbourg Cedex (France)
Fax: (+33) 368851637
E-mail: jpsauvage@unistra.fr

[b] Dr. J.-P. Sauvage
Present address: ISIS, 8 allée Gaspard Monge
University of Strasbourg, 67000 Strasbourg (France)

2,6-di(8′-phenylisoquinolin-3′-yl)pyridine (dpiq-py; see Scheme 1). By complexing two such compounds to an octahedral transition-metal centre (Ru^{II}, Fe^{II} or Co^{III}), an entanglement is formed that contains two highly entwined organic fragments, with no strain or congestion around the metal, thanks to the non-sterically hindering nature of the ligands. From the entanglement obtained, [2]catenanes can be prepared in high yield.

Results and Discussion

Design: Although complexes containing two 6,6″-diphenyl-2,2′:6′,2″-terpyridine (dp-terpy) fragments coordinated to a transition metal may appear to be attractive targets to generate entanglements, the dp-terpy ligand is not well adapted to the formation of entwined complexes due to the steric repulsion between the aromatic groups borne by the first terpyridine nucleus and the terpyridine core of the second dp-terpy unit. By coordination to a metal centre, this problem is made even more acute by the "pinching effect" originating from coordination of the three pyridine nuclei of a terpy ligand. This problem is illustrated in Scheme 1. The main reason for the steric congestion found in $[M(dp\text{-}terpy)_2]^{n+}$ complexes (M = octahedral transition-metal centre) is simply that the angles between the axes of the three pyridine nuclei are not the same in the free ligand as in its complexes. Due to coordination to the metal atom, each terpy ligand is "pinched" and the two phenyl-ring axes are no longer parallel, which creates steric repulsion as indicated in Scheme 1. As shown many years ago, dp-terpy is unable to form stable $[M(dp\text{-}terpy)_2]^{n+}$ complexes.[40–41] The only example that has been found is the ruthenium(II) complex $[Ru(dp\text{-}terpy)_2]^{2+}$, which seems to be stable in the dark but undergoes an efficient photochemical ligand-substitution reaction, leading to release of strain by de-coordinating the two lateral pyridine nuclei from the metal upon irradiation with light.[41] Owing to a complete lack of steric hindrance between the various parts of the complex, the new ligand dpiq-py is perfectly adapted to the formation of entanglements consisting of two tridentate aromatic ligands for which the coordination mode is similar to that of terpy.

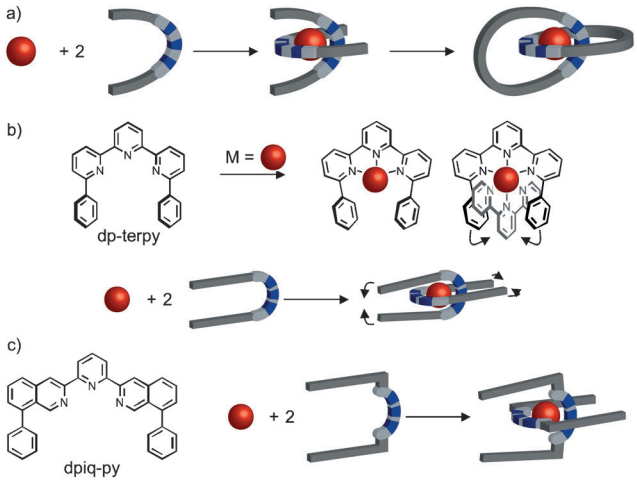

Scheme 1. a) Generation of a two-component entanglement and synthesis of a [2]catenane based on tridentate ligands and an octahedral transition metal as the template; b) By coordination to a metal centre M, the whole ligand structure is pinched and the two phenyl rings of the dp-terpy chelating compound come closer together. As a consequence, severe steric repulsion occurs between various aromatic fragments within the complex; c) In contrast, even if the same "pinching" process is observed when coordinating a dpiq-py ligand to a metal, the distance between the two phenyl rings of the same ligand is such that there is no steric repulsion with the other ligand, making the corresponding complexes highly stable. In addition, the entanglement is particularly well adapted to the formation of a [2]catenane, because the extremities of each tridentate chelating group are located considerably beyond the metal centre, forcing the two future rings to be interlocked with one another.

Acyclic precursors and analogues: Our goal was first to synthesise a tridentate ligand containing two anisyl groups. These two substituents can subsequently be modified to give a cyclised ligand when coordinated to a metallic centre. The tridentate ligand 2,6-di[8′-(*para*-anisyl)isoquinolin-3′-yl]pyridine **4** was prepared in two steps (Scheme 2) from anisyltriflate derivative **1**.[39] Substitution of the triflate group with a trimethylstannane group was performed with hexamethylditin in the presence of $[Pd(PPh_3)_4]$ as the catalyst and potassium iodide, which inhibits reductive elimination of the OTf functional group. The expected product **2** was obtained in 80% yield. A Stille cross-coupling of compound **2** with diiodopyridine **3** in the presence of $[Pd(PPh_3)_4]$ gave tridentate ligand **4** in 58% yield.

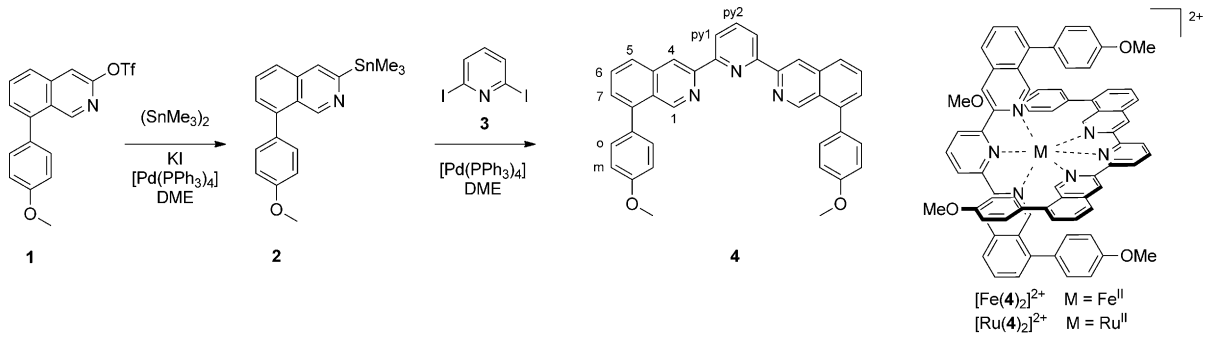

Scheme 2. Synthesis of ligand **4** and the corresponding Fe^{II} and Ru^{II} complexes

The coordination chemistry of the new ligand **4** was then studied with iron(II) and ruthenium(II) salts. Complexation with $[Fe(BF_4)_2]$ was performed at room temperature and the red complex $[Fe(\mathbf{4})_2)][PF_6]_2$ was obtained quantitatively after purification by silica gel column chromatography. The complexation reaction with Ru^{II} needed harsher conditions. Thus, it was performed in ethylene glycol under microwave irradiation And the product was purified by silica gel column chromatography, providing the dark red complex $[Ru(\mathbf{4})_2)][PF_6]_2$ in 75% yield. The ^{1}H NMR spectra for the two complexes showed typical chemical shifts for the protons, characteristic of the complexation of two entwined ligands around the metal centre.

Crystals of the iron(II) complex suitable for X-ray crystallography were grown by diffusion of isopropyl ether in acetone. No strong stacking interactions have been observed between two neighbouring molecules in the unit cell. The X-ray structure (Figure 1) gives information about the octahedral environment of the iron(II) metal centre, and about the strong pinching of the ligands (2,6-di[8′-(*para*-anisyl)isoquinolin-3′-yl]pyridine) around the metal centre.

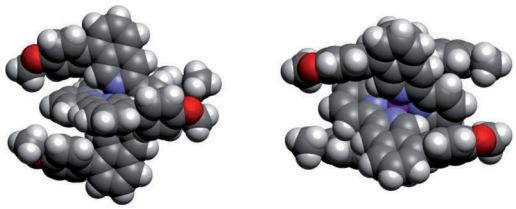

Figure 1. Different views of the X-ray structure of $[Fe(\mathbf{4})_2][PF_6]_2$. Atoms in the second half of the molecule are related to the first by inversion through a centre of symmetry.

The coordination sphere around the Fe^{II} centre is slightly distorted. The distances between the N atoms and the iron atom are more or less normal (see Table 1). As expected, the central atom of each tridentate ligand is significantly closer to the Fe atom than the peripheral N atoms (1.883 Å and 1.975 Å, respectively). The $N_{central}$-Fe-$N_{central}$ atom angle is close to ideal (178.92°), whereas the $N_{peripheral}$-Fe-$N_{peripheral}$ angle is, as expected, much smaller than that of an ideal octahedron (162.82°).

Finally, and probably particularly importantly, coordination of a metal, such as Fe^{II}, to ligand **4** induces a very strong "pinching" of the organic backbone, bringing the two oxygen atoms in each ligand into close proximity (8.536 Å). The angle between the two anisyl-ring axes (each axis is defined as the straight line joining the oxygen atom borne by the phenyl ring and the carbon atom *para* to this O atom, MeO-Ph-) is roughly equal to 19°. Remarkably, this significant distortion, which will of course facilitate intra-ligand cyclisation reactions, does not lead to any constraint around the metal centre because the aromatic groups involved (anisyl groups) are attached to the tridentate ligand at positions that are remote from the metal coordination sphere.

Table 1. Comparison of selected bond lengths [Å] and angles [°] within the coordination spheres of $[Fe(\mathbf{4})_2)][PF_6]_2$ and $[Fe(\mathbf{9})][PF_6]_2$.

	$[Fe(\mathbf{4})_2)][PF_6]_2$	$[Fe(\mathbf{9})][PF_6]_2$[a]
Fe–N bond lengths		
with the central N atoms	1.883	1.879
with the lateral N atoms	1.975	1.980
axial N-Fe-N angles		
with the central N atoms	178.92	179.15
with the lateral N atoms	162.82	161.82
intra-ligand O–O separations	8.536	8.010
		8.300

[a] Average values.

Fe^{II} and Co^{III} complexed [2]catenanes:

Synthesis of tridentate ligand ***7****; the precursor to the catenane*: Tridentate ligand **7** was prepared in two steps from ligand **4** (Scheme 3). Deprotection of the anisyl groups in ligand **4**, by using pyridinium chloride and microwave irradiation at ambient pressure, gave diphenol **5** in a quantitative yield. A double Williamson reaction between diphenol **5** and the tosylated chain (2-allyloxyethoxy)tosylsulfonate (**6**, obtained in a one-step reaction from commercially available allyloxyethanol) gave ligand **7** in 72% yield.

Synthesis of the Fe^{II} *complexes*: Ligand **7** was treated with half an equivalent of iron(II) ions to generate the octahedral complex $[Fe(\mathbf{7})_2]^{2+}$ (Figure 2). After addition of an excess of saturated aqueous KPF_6 solution, the precursor complex was obtained as its hexafluorophosphate salt in 92% yield. ^{1}H NMR spectroscopy provided clear evidence that the complex is diamagnetic. It also presented ^{1}H chemical shifts characteristic of octahedral complexes containing two entwined ligands. In particular protons H_1, adjacent to the isoquinolyl nitrogen atoms, are shifted upfield by about 1.75 ppm upon complexation (Figure 3). This observation is in agreement with the formation of a complex in which the

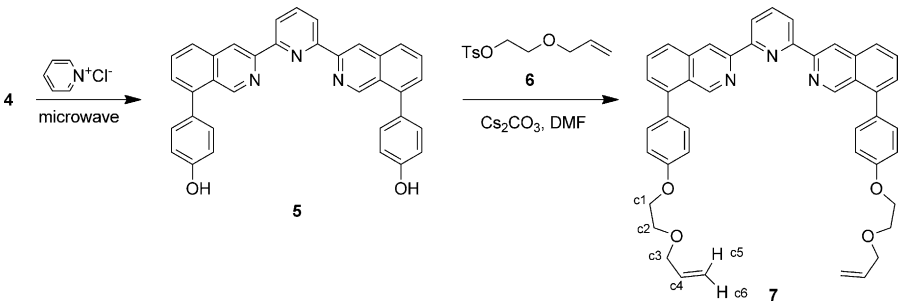

Scheme 3. Synthesis of the tridentate ligand **7**.

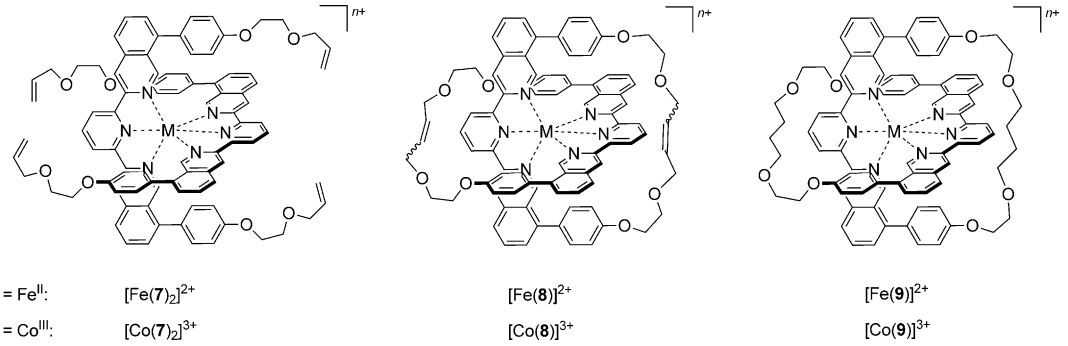

Figure 2. Fe^{II} and Co^{III} acyclic complexes and catenanes.

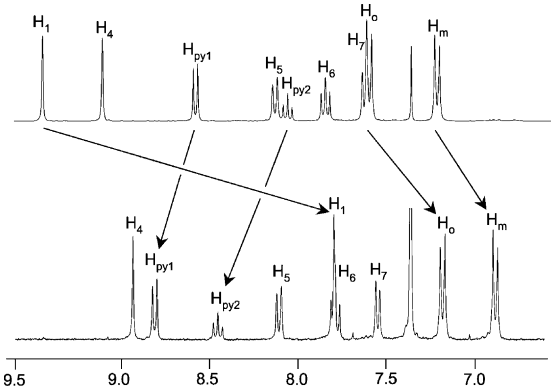

Figure 3. ^1H NMR spectra of ligand **7** (top) and complex $[Fe(\mathbf{7})_2]^{2+}$ (bottom) in $CDCl_3$. The numbering scheme is shown in Schemes 2 and 3.

H_1 protons are located in the shielding cone of the central pyridine ring of the opposite ligand.

Cyclisation of this precursor complex by ring-closing metathesis (RCM) of its terminal olefins was performed in dichloromethane at room temperature in the presence of the first-generation Grubbs catalyst.[42] The double ring-closure reaction gave catenane $[Fe(\mathbf{8})]^{2+}$ as a dark-red solid in 75% yield after purification by column chromatography on alumina. The signals for the terminal olefins (6.13, 5.48 and 5.34 ppm) disappeared, whereas those for cyclic olefins appeared at 6.19 and 6.08 ppm as a mixture of *cis* (88%) and *trans* (12%) isomers, integrating for four protons.

The catenane $[Fe(\mathbf{8})]^{2+}$ was then hydrogenated under an H_2 atmosphere with Pd/C (10 mol% Pd) as the catalyst, in a 1:1 mixture of CH_2Cl_2 and EtOH at room temperature. The purified reduced catenane $[Fe(\mathbf{9})]^{2+}$ was obtained in 99% yield, as its PF_6 salt. ^1H NMR spectroscopy showed the complete disappearance of the olefinic signals and appearance of two new signals at 3.86 and 1.99 ppm, corresponding to the new methylene protons.

The molecular structure of the iron(II) catenane $[Fe(\mathbf{9})][PF_6]_2$ was confirmed by X-ray crystallography (Figure 4). The crystal was a racemic twin, as suggested by the Flack parameter of 0.55(2). The catenane has roughly the same coordination sphere as the entwined precursor. The main difference lies in the pinching effect. The angle between the two "anisyl" ring axes (each axis is defined as the straight line joining the oxygen atom borne by the phenyl ring and the carbon atom *para* to this O atom) is roughly equal to 23°, that is, very strongly pinched. It appears to be more pinched than in the open system $[Fe(\mathbf{4})_2)][PF_6]_2$ ("entwined complex"), which indicates that cyclisation has an effect on the geometry and brings the two oxygen atoms borne by the lateral aromatic groups closer to one another (see Table 1 and Figure 1). Interestingly, one of the ligands is significantly more pinched than the other (O–O separations of 8.010 and 8.300 Å, respectively). As for the precursor, the two -O-Ph- fragments are too far away to perturb the coordination sphere of the Fe^{II} centre.

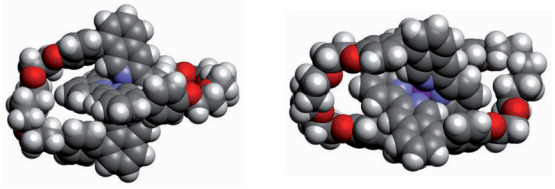

Figure 4. X-ray crystal structure of $[Fe(\mathbf{9})][PF_6]_2$.

Synthesis of the Co^{III} complexes: Because ligand exchange around Co^{III} centres is very slow and difficult, it is common to assemble the ligands around Co^{II} ions and then lock the system by oxidation to Co^{III}. Reaction of ligand **7** with a cobalt(II) salt, followed by oxidation with cerium(IV) and anion exchange with KPF_6 afforded the octahedral complex $[Co(\mathbf{7})_2][PF_6]_3$ (Figure 2) in 72% yield as an orange solid. The ^1H NMR spectrum of $[Co(\mathbf{7})_2]^{3+}$ is sharp and well resolved, showing a low-spin and diamagnetic state, as expected for Co^{III}–polypyridine derivatives. As for the analogous iron complex $[Fe(\mathbf{7})_2]^{2+}$, the ^1H NMR spectrum showed that protons H_1 adjacent to the nitrogen atoms are strongly shifted upfield, which is a signature of the entwined structure of the corresponding complex.

The double ring-closing metathesis, performed under the same reaction conditions as for the iron(II) analogue, was incomplete and extra Grubbs catalyst was necessary to close the two rings. Furthermore, the cobalt ions were partially reduced during this metathesis reaction, it was, thus, necessary to treat the solution with Ce^{IV} at the end of the RCM reac-

tion to obtain the Co^{III} catenane. Purification by chromatography on alumina and anion exchange with KPF_6 afforded the catenane $[Co(\mathbf{8})][PF_6]_3$ as a yellow powder in 70% yield. The ^1H NMR spectrum showed two signals corresponding to the *cis* and *trans* olefinic protons, in a 3:1 ratio.

Reduction of the double bonds under the usual conditions was also incomplete. Hydrogenation of the double bonds with H_2 required equimolar quantities of the Pd/C catalyst. As in the RCM reaction, the resulting solution was the treated with Ce^{IV}. This oxidation reaction was followed by anion exchange with KPF_6 to afford the final catenane $[Co(\mathbf{9})][PF_6]_3$ in 60% yield.

The electrospray mass spectrum of each Co^{III} complex showed a peak corresponding to $[M-3PF_6]^{3+}$. A second peak corresponding to $[M-2PF_6]^{2+}$, the intensity of which was not negligible, was also present, although the NMR spectrum showed that these complexes were fully diamagnetic. The Co^{II} peaks probably originate from partial reduction of the complex in the mass spectrometer source.[43]

Physical properties:

Electrochemistry: The redox behaviour of complexes $[Ru(\mathbf{4})_2]^{2+}$, $[Fe(\mathbf{4})_2]^{2+}$, $[Fe(\mathbf{9})]^{2+}$ and $[Co(\mathbf{9})]^{3+}$ was analysed by using cyclic voltammetry. The redox potentials of the various complexes are collected in Table 2, the ligand-based reduction processes could only be observed on the anodic sweep, with very poorly resolved waves. The return peaks were generally masked by intense adsorption waves. The four complexes show typical reversible metal-centred redox processes, in agreement with the literature data (see Table 2). As expected, the electrochemical properties are mainly ruled by the choice of metal and only very weakly by the ligand. Indeed, the ruthenium(II) complex shows a reversible oxidation wave around 1.2 V, and the Fe^{III}/Fe^{II} redox potentials are observed around 1.1 V. By contrast, the Co^{III}/Co^{II} potential is observed at a much lower value ($E_{1/2}=$ 0.18 V vs. SCE), in accordance with other cobalt polypyridine compounds.[19,44,45]

Table 2. Electrochemical data versus SCE.[a]

	M^{3+}/M^{2+} [V] (ΔE_p [mV])		M^{3+}/M^{2+} [V]
$[Ru(\mathbf{4})_2]^{2+}$	1.17 (82)	$[Ru(dqpy)_2]^{2+}$	1.14[47]
$[Fe(\mathbf{4})_2]^{2+}$	1.07 (60)	$[Ru(terpy)_2]^{2+}$	1.28[46]
$[Fe(\mathbf{9})]^{2+}$	1.08 (73)	$[Fe(terpy)_2]^{2+}$	1.13[44,48]
$[Co(\mathbf{9})]^{3+}$	0.18 (85)	$[Co(terpy)_2]^{3+}$	0.16[19,44,45]

[a] Oxidation potentials (vs. SCE) measured by cyclic voltammetry of the Ru^{II}, Fe^{II} and Co^{III} complexes. Conditions for the four new complexes: acetonitrile/dichloromethane (9:1), against $Ag^+/AgCl$ electrode and referenced to ferrocene as 0.5 V, by using 0.1 M nBu_4NPF_6 as the electrolyte, $\nu=200$ mV s^{-1}.

The cyclic voltammograms of the ruthenium and iron complexes show one or two irreversible one-electron reduction peaks around −1.40 V. These can be assigned to ligand-based reductions.[48] The cobalt complex shows a quasi-reversible one-electron reduction wave at −0.87 V, which formally corresponds to the Co^{II}/Co^{I} process.[45]

UV/Vis absorption spectroscopy: The UV/Vis absorption spectra of the complexes $[Ru(\mathbf{4})_2]^{2+}$, $[Fe(\mathbf{4})_2]^{2+}$, $[Fe(\mathbf{9})]^{2+}$ and $[Co(\mathbf{9})]^{3+}$ are depicted in Figure 5. The absorption maxima and molar absorption coefficients are collected in Table 3. The absorption spectra of the complexes are characterised by three distinct zones: 1) the ultraviolet region below 300 nm shows intense bands that can be assigned to $^1\pi$–π^* ligand-centred transitions; 2) various absorption bands are observed in the region between 300 and 400 nm,[50] which are likely to correspond to ^{1}n–π^* and intraligand charge-transfer (^{1}ILCT) transitions; and 3) the absorption bands in the visible region of the spectra are assigned to metal-to-ligand charge-transfer (MLCT) bands, in agreement with previous reports on related complexes.[19,51] Although the classical $[Ru(terpy)_2]^{2+}$ chromophore shows one MLCT band centred at 475 nm,[46] it is interesting to

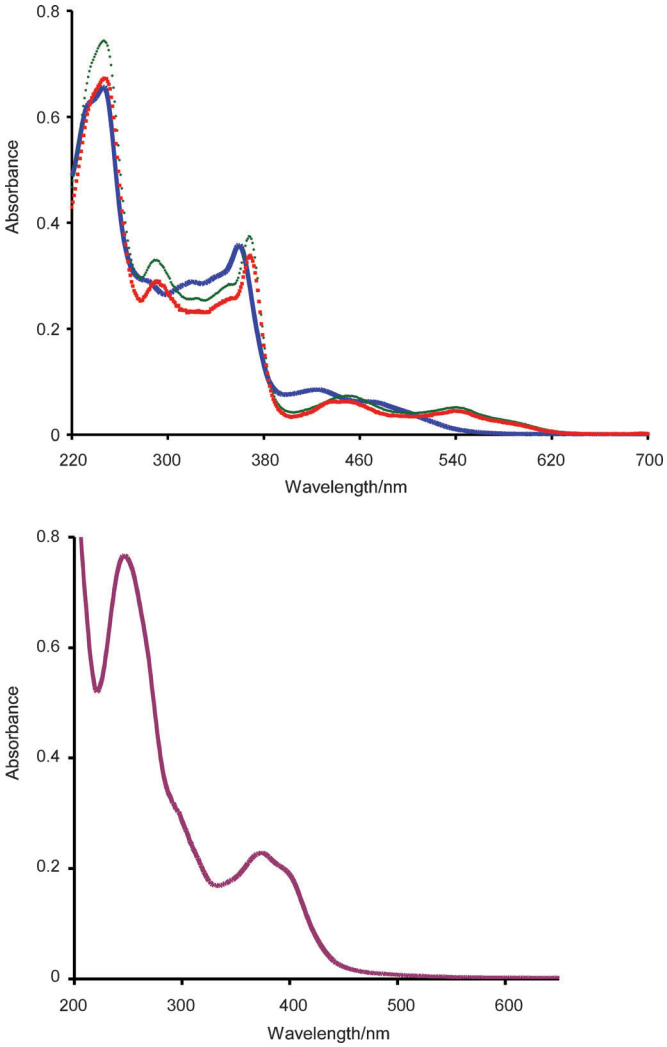

Figure 5. UV/Vis absorption spectra of the complexes $[Ru(\mathbf{4})_2]^{2+}$ (blue), $[Fe(\mathbf{4})_2]^{2+}$ (red), $[Fe(\mathbf{9})]^{2+}$ (green) and $[Co(\mathbf{9})]^{3+}$ (purple) in acetonitrile at room temperature.

Table 3. Absorption data in acetonitrile for the four complexes, at room temperature.

	λ_{max} [nm] (ε [$M^{-1}cm^{-1}$])				
$[Ru(\mathbf{4})_2]^{2+}$	246 (69900)	317 (30600)	359 (38100)	426 (9000)	466 (6700)
$[Fe(\mathbf{4})_2]^{2+}$	247 (89100)	291 (38400)	368 (44800)	449 (8700)	541 (6100)
$[Fe(\mathbf{9})]^{2+}$	248 (70600)	290 (30200)	369 (35000)	451 (6600)	542 (4700)
$[Co(\mathbf{9})]^{3+}$	247 (132400)	–	374 (39500)	–	–

note that complex $[Ru(\mathbf{4})_2]^{2+}$ shows two MLCT bands at 466 and 426 nm. The same feature is observed for the iron(II) analogue. Furthermore, the MLCT bands for the iron(II) complexes appear redshifted with respect to the ruthenium complex, which is in agreement with previous reports on related complexes[50] and which simply indicates that Fe^{II} is easier to oxidise than Ru^{II}. The cobalt(III) complex shows an absorption band at 374 nm, the exact nature of which is uncertain. These absorptions are responsible for the orange colour of the complex, and their wavelength corresponds to that observed in the literature.[19,52]

Conclusion

Ligands derived from 2,6-di(8′-*para*-anisylisoquinolin-3′-yl)-pyridine are particularly well adapted to the formation of highly stable entwined complexes with octahedral transition metal centres. These aromatic compounds constitute an alternative to the terpy tridentate chelate that, in contrast to the present series of molecules, cannot form entangled complexes when substituted at the nitrogen atom α positions due to steric repulsion. Interestingly, in spite of the strongly pinched geometry of the coordinated ligands, there is no significant steric hindrance between the lateral aromatic fragments borne by a given chelate and the coordinating core of the other ligand. The reason for this is that the distance between the two attachment points of the lateral groups onto the tridentate unit itself is very large (c.a. 10.5 Å), which allows distortion without repulsion. The new tridentate ligand described in this report and the corresponding macrocycles incorporating this unit will be used to elaborate future molecular machines based on 5-coordinate or octahedral transition-metal centres.

Experimental Section

General: Some solvents were distilled over the appropriate drying agent: tetrahydrofuran and diethyl ether over sodium and benzophenone, dichloromethane over calcium hydride, and triethylamine over potassium hydroxide. Anhydrous DMF was used as received. Thin-layer chromatography (TLC) was performed by using glass sheets coated with silica or neutral alumina. Column chromatography was carried out on silica gel (Kieselgel 60, 0.063–0.200 mm, Merck) or alumina (aluminium oxide 90 standardised or acid, 0.063–0.200 mm, Merck). All reactions were carried out under an argon atmosphere and in oven-dried glassware. 8-(*para*-Anisyl)isoquinolin-3-yl trifluoromethanesulfonate **1** was synthesised according to a procedure described previously by our group.[39]

Instrumentation: Proton nuclear magnetic resonance (^{1}H NMR and 2D COESY) spectra were acquired on either a Bruker AVANCE 300 (300 MHz), a Bruker AVANCE 400 (400 MHz) or a Bruker AVANCE 500 (500 MHz) spectrometer. 2D ROESY spectra were measured by using a Bruker AVANCE 500 (500 MHz) spectrometer. The spectra were referenced to residual protonated solvent references (^{1}H: $CDCl_3$: 7.24; CD_3CN: 1.94; [D$_6$]DMSO: 2.50; CD_2Cl_2: 5.32 ppm). Mass spectra were obtained by using a Bruker MicroTOF (MS (ES)) spectrometer or a Bruker Daltonics autoreflex II TOF/TOF spectrometer with dithranol as the matrix (MALDI). UV/Vis absorption spectra were performed by using a Kontron UVIKON 860 spectrophotometer. Cyclic voltammetry experiments were performed by using an EG&G Princeton Applied Research 273 A potentiostat, a Pt working electrode, a Pt wire as a counter electrode, a silver wire as a pseudo-reference electrode and a 0.1 M solution of Bu_4NPF_6 in MeCN/CH_2Cl_2 (9:1) as the supporting electrolyte. Potentials are quoted versus the ferrocene/ferricenium couple ($E_0(Fc^+/Fc^0)=0.4$ V vs. SCE) and all the redox potentials were referenced to internal ferrocene added at the end of each experiment.

X-ray structure solution and refinement: Single-crystal X-ray diffraction experiments were carried out by the service of the University of Strasbourg (Dr. Lydia Brelot). The crystals were placed in oil, and a single crystal was selected, mounted on a glass fibre and placed in a low-temperature N_2 stream. CCDC-847292 ($[Fe(\mathbf{4})_2][PF_6]_2$) and CCDC-847293 ($[Fe(\mathbf{9})][PF_6]_2$) contain the supplementary crystallographic data for this paper. These data can be obtained free of charge from The Cambridge Crystallographic Data Centre via www.ccdc.cam.ac.uk/data_request/cif.

Conditions for the entwined iron(II) complex: X-ray diffraction data collection was carried out on a Nonius Kappa-CCD diffractometer equipped with an Oxford Cryosystem liquid N_2 device by using $Mo_{K\alpha}$ radiation ($\lambda=0.71073$ Å). The crystal–detector distance was 36 mm. The cell parameters were determined (Denzo software)[53] from reflections taken from one set of 10 frames (1.0° steps in phi angle), each at 20 s exposure. The structure was solved by direct methods using the program SHELXS-97.[54] The refinement and all further calculations were carried out by using SHELXL-97.[55] The H atoms were included in calculated positions and treated as riding atoms by using SHELXL default parameters. The non-H atoms were refined anisotropically by using weighted full-matrix least-squares on F^2. One of the methyl groups is disordered over two positions. The SQUEEZE instruction in PLATON[56] was applied. The residual electron density was assigned to one molecule of acetone and one molecule of isopropyl ether. The structures were drawn by using Mercury.

Conditions for the entwined iron(II) catenane: X-Ray diffraction data collection was carried out on a Bruker APEX II DUO Kappa-CCD diffractometer equipped with an Oxford Cryosystem liquid N_2 device by using $Mo_{K\alpha}$ radiation ($\lambda=0.71073$ Å). The crystal–detector distance was 38 mm. The cell parameters were determined (APEX2 software)[5] from reflections taken from three sets of 12 frames, each at 10 s exposure. The structure, refinement and calculations were solved as described above. A semi-empirical absorption correction was applied by using SADABS in APEX2;[57] transmission factors: $T_{min}/T_{max}=0.6582/0.7456$. The structure was treated as a racemic twin solved within the $P2_12_12_1$ space group with a BASF of 0.54975.

[8-(*para*-Anisyl)isoquinolin-3-yl]trimethylstannane (2): Compound **1** (437 mg, 1.14 mmol) was placed in a two-necked round-bottom flask (50 mL) in the presence of hexamethyldistannane (747 mg, 2.28 mmol), potassium iodide (378.5 mg, 2.28 mmol) and tetrakis(triphenylphosphine)palladium(0) (63.6 mg, 0.057 mmol). Dimethoxyethane (24 mL) was then added and the reaction was heated at reflux (90 °C) for 18 h. After cooling and evaporation of the solvents (stannyl byproducts were neutralised with KOH in ethanol), the resulting residue was dissolved in diethyl ether and impurities were filtered off. The solvent was evaporated and compound **2** was obtained as a yellow oil (363 mg, 80 %). ^{1}H NMR ($CDCl_3$, 300 MHz): $\delta=9.44$ (s, 1H), 7.82 (fine d, 1H, $J=1.1$ Hz), 7.69 (s, 1H), 7.67 (dd, 1H, $J=7.4$, 6.7 Hz), 7.44 (dd, 1H, $J=7.4$, 1.7 Hz), 7.41 (d, 2H, $J=8.8$ Hz), 7.02 (d, 2H, $J=8.8$ Hz), 3.87 (s, 3H), 0.38 ppm (s, 9H).

2,6-Di[8′-(*para*-anisyl)isoquinolin-3′-yl]pyridine (4): 2,6-Diiodopyridine (**3**; 63 mg, 0.27 mmol), tetrakis(triphenylphosphine)palladium(0) (37 mg,

0.033 mmol) and stannyl derivative **2** (217 mg, 0.55 mmol) were placed in a two-necked round-bottom flask (50 mL) and dissolved in toluene (11 mL). The resulting mixture was heated at reflux for 24 h. The solvents were evaporated (stannyl byproducts were neutralised with KOH in ethanol) and the residue was dissolved in dichloromethane. Distilled water was added and the organic phase was separated off. The aqueous phase was extracted twice with CH_2Cl_2. The combined organic phases were evaporated and the residue purified by chromatography on Al_2O_3 by using dichloromethane/pentane (2:1) as the eluent to afford pure compound **8** as a white solid (85 mg, 58%). ^{1}H NMR ($CDCl_3$, 300 MHz): δ = 9.46 (s, 2H; H_1), 9.10 (s, 2H; H_4), 8.54 (d, 2H, J = 7.8 Hz; H_{py1}), 8.07 (d, 2H, J = 8.1 Hz; H_5), 8.00 (t, 1H, J = 7.8 Hz; H_{py2}), 7.77 (dd, 2H, J = 7.2, 7.2 Hz; H_6), 7.54 (d, 2H, J = 7.2 Hz; H_7), 7.51 (d, 4H, J = 8.6 Hz; H_o), 7.08 (d, 4H, J = 8.6 Hz; H_m), 3.91 ppm (s, 6H; H_{Me}); MALDI-MS: m/z calcd for $C_{37}H_{27}N_3O_2$: 545.2182; found: 545.476.

[Fe(4)$_2$][PF$_6$]$_2$: Ligand **4** (16 mg, 0.029 mmol) was placed in a round-bottom flask (25 mL) under argon and (partially) dissolved in dichloromethane (5 mL). A solution of $[Fe(BF_4)_2]\cdot 6H_2O$ (4.9 mg, 0.015 mmol) in acetonitrile (3 mL) was added and the solution was stirred at room temperature for 2 h. After this time, all solvents were evaporated and the residue was purified by column chromatography on SiO_2 with acetone/H_2O/KNO_3 (100:5:0.2; saturated solution of KNO_3) as the eluent. After an anion exchange reaction, [Fe(**4**)$_2$][PF$_6$]$_2$ was obtained as a red solid (21 mg, 99%). Crystals were obtained by diffusion of diisopropyl ether in acetone. ^{1}H NMR (CD_2Cl_2, 500 MHz): δ = 9.28 (s, 4H; H_4), 9.15 (d, 4H, J = 8.1 Hz; H_{py1}), 8.67 (t, 2H, J = 8.1 Hz; H_{py2}), 8.05 (s, 4H; H_1), 8.04 (d, 4H, J = 7.0 Hz; H_5), 7.80 (dd, 4H, J = 7.0, 7.0 Hz; H_6), 7.53 (d, 4H, J = 7.0 Hz; H_7), 7.10 (d, 8H, J = 8.6 Hz; H_o), 6.98 (d, 8H, J = 8.6 Hz; H_m), 4.09 ppm (s, 12H; H_{Me}); MS (ES): m/z calcd for $[C_{74}H_{54}N_6O_4Fe+H^+]$: 573.1774 [$M$+H$^+$]; found: 573.1643.

[Ru(4)$_2$][PF$_6$]: Ligand **4** (10 mg, 0.018 mmol) and $[RuCl_2(dmso)_4]$ (4.4 mg, 0.009 mmol) were placed in a pear-shaped flask (5 mL) under argon and ethylene glycol (3 mL) was added. The mixture was then heated in a microwave oven (three times 5 min with maximum power 500 W). A saturated solution of KPF_6 in water (15 mL) was then added, and the precipitate formed was filtered and washed copiously with water. The residue was purified by chromatography on SiO_2 with acetone/H_2O/KNO_3 (50:5:0.5; saturated solution of KNO_3) as the eluent. After an anion exchange reaction, [Ru(**4**)$_2$][PF$_6$]$_2$ was obtained as a dark-red solid (10 mg, 75%). Crystals were obtained by slow diffusion of diisopropyl ether in acetone. ^{1}H NMR ([D$_6$]acetone, 300 MHz): δ = 9.37 (s, 2H; H_4), 9.09 (d, 4H, J = 8.1 Hz; H_{py1}), 8.57 (t, 2H, J = 8.1 Hz; H_{py2}), 8.31 (s, 4H; H_1), 8.11 (d, 4H, J = 8.2 Hz; H_5), 7.86 (dd, 4H, J = 8.2, 7.4 Hz; H_6), 7.61 (d, 4H, J = 7.4 Hz; H_7), 7.06 (d, 8H, J = 9.4; H_o), 7.03 (d, 8H, J = 9.4; H_m), 4.05 ppm (s, 12H; H_{Me}); MS (ES): m/z calcd for $[C_{74}H_{54}N_6O_4Ru+H^+]$: 596.1630 [$M$+H$^+$]; found: 596.1748.

2,6-Di(8′-(*para*-hydroxyphenyl)isoquinolin-3′-yl)pyridine (5): A large excess of pyridinium chloride (around 50 equiv) was added to compound **4** (230 mg, 0,42 mmol) in a round-bottom flask. The reaction mixture was heated at reflux with a microwave oven for 10 min. The heating was carried out twice more after addition of the same amount of pyridinium chloride. The solid residue was taken up with water (50 mL) and the solution was neutralised to pH 7–8 by using 33% aqueous ammonium hydroxide. The suspension was then filtered and washed with water. The recovered solid was dried under vacuum overnight to give pure compound **5** (213 mg, 98%). ^{1}H NMR (DMSO, 300 MHz): δ = 9.39 (s, 2H; H_1), 9.35 (s, 2H; H_4), 8.58 (d, 2H, J = 7.9 Hz; H_{py1}), 8.28 (d, 2H, J = 8.1 Hz; H_5), 8.19 (t, 1H, J = 7.9 Hz; H_{py2}), 7.97 (dd, 2H, J = 7.5, 7.5 Hz; H_6), 7.66 (d, 2H, J = 7.0 Hz; H_7), 7.49 (d, 4H, J = 8.6 Hz; H_o), 7.02 ppm (d, 4H, J = 8.6 Hz; H_m).

(2-Allyloxyethoxy)-*para*-toluenesulfonate (6): 2-Allyoxyethanol (0.27 mL, 0.253 g, 2.48 mmol), 4-dimethylaminopyridine (18.2 mg, 0.15 mmol) and triethylamine (1.72 mL, 1.25 g, 12.38 mmol) were dissolved in dry dichloromethane (10 mL). After cooling to 0°C, *para*-toluenesulfonyl chloride (1.18 g, 6.19 mmol) was added in small portions to the reaction mixture. The mixture was then allowed to warm to room temperature overnight. The reaction mixture was acidified to pH 3 with 10% aqueous HCl and the product was extracted with dichloromethane. The combined organic layers were dried and evaporated. The residue was purified by chromatography on silica gel by using dichloromethane/methanol (100:0 to 100:2) as the eluent. Compound **6** was obtained as a yellow oil (603 mg, 95%). ^{1}H NMR ($CDCl_3$, 300 MHz): δ = 7.81 (d, 2H, J = 8.2 Hz), 7.35 (d, 2H, J = 8.1 Hz), 5.82 (m, 1H), 5.18 (m, 1H), 4.17 (t, 2H, J = 4.7 Hz), 3.95 (td, 2H, J = 5.7, 1.46 Hz), 3.62 ppm (t, 2H, J = 4.9 Hz); MS (ES): m/z calcd for $C_5H_{10}O_2Na$: 125.057 [M+Na$^+$]; found: 125.056.

2,6-Di[8′-(*para*-allyloxyethoxyphenyl)isoquinolin-3′-yl]pyridine (7): Compound **5** (60 mg, 0.116 mmol) and Cs_2CO_3 (226 mg, 0.696 mmol) were dissolved in dry DMF (5 mL). The solution was stirred at 60°C for 30 min. Compound **6** (90 mg, 0,548 mmol) was added and the mixture was heated to 75°C for 16 h. The solvent was evaporated and the residue dissolved in dichloromethane. Distilled water was added and the organic phase was separated off. The aqueous phase was extracted twice with CH_2Cl_2. The combined organic phases were evaporated and the residue purified by chromatography on Al_2O_3 by using dichloromethane/pentane (3:2 to pure dichloromethane) as the eluent to give **7** as a white solid (57 mg, 72%). ^{1}H NMR ($CDCl_3$, 300 MHz): δ = 9.47 (s, 2H; H_1), 9.11 (s, 2H; H_4), 8.55 (d, 2H, J = 7.8 Hz; H_{py1}), 8.08 (d, 2H, J = 8.1 Hz; H_5), 8.01 (t, 1H, J = 7.9 Hz; H_{py2}), 7.79 (dd, 2H, J = 7.6, 7.2 Hz; H_6), 7.57 (d, 2H, J = 7.2 Hz; H_7), 7.53 (d, 4H, J = 8.8 Hz; H_o), 7.13 (d, 4H, J = 8.8 Hz; H_m), 6.00 (ddt, 2H, J = 16.5, 10.5, 5.4 Hz; H_{c4}), 5.35 (dd, 2H, J = 16.5, 1.5 Hz; H_{c5}), 5.25 (dd, 2H, J = 10.5, 1.4 Hz; H_{c6}), 4.26 (t, 4H, J = 5.0; H_{c1}), 4.16 (d, 4H, J = 5.4 Hz; H_{c3}), 3.89 ppm (t, 4H, J = 5.0 Hz; H_{c2}); MS (ES): m/z calcd for $C_{45}H_{39}N_3O_4$: 686.301 [M+H$^+$]; found: 687.252.

[Fe(7)$_2$][PF$_6$]$_2$: Compound **7** (47 mg, 0.069 mmol) was placed in a round-bottom flask (25 mL) and dissolved in dichloromethane (11 mL). A solution of $[Fe(BF_4)_2]\cdot 6H_20$ (11.6 mg, 0.0343 mmol) in acetonitrile (7 mL) was added and the reaction was stirred at room temperature for 2 h. After this time, all solvents were evaporated and the residue was purified by chromatography on Al_2O_3 by using dichloromethane/methanol (100:4) as the eluent. After evaporation of the collected fractions, the solid was dissolved in dichloromethane, a saturated aqueous solution of KPF_6 (4 mL) was added, the organic solvent was evaporated and the precipitate was collected by filtration. The compound [Fe(**7**)$_2$][PF$_6$]$_2$ was obtained as a red solid (54.7 mg, 92%). ^{1}H NMR ($CDCl_3$, 300 MHz): δ = 8.92 (s, 4H; H_4), 8.79 (d, 4H, J = 8.1 Hz; H_{py1}), 8.41 (t, 2H, J = 8.1 Hz; H_{py2}), 8.04 (d, 4H, J = 8.4 Hz; H_5), 7.72 (m, 8H; H_1, H_6), 7.45 (d, 4H, J = 7.2 Hz; H_7), 7.08 (d, 8H, J = 8.6 Hz; H_o), 6.77 (d, 8H, J = 8.6 Hz; H_m), 6.13 (ddt, 4H, J = 17.2, 10.8, 5.7 Hz; H_{c4}), 5.48 (dd, 4H, J = 17.2, 1.3 Hz; H_{c5}), 5.34 (d, 4H, J = 10.8 Hz; H_{c6}), 4.51 (m, 8H; H_{c1}), 4.31 (d, 8H, J = 5.7 Hz; H_{c3}), 4.09 ppm (m, 8H; H_{c2}); MS (ES): m/z calcd for $C_{90}H_{78}N_6O_8Fe$: 713.261 [M/2]; found: 713.238.

[Fe(8)][PF$_6$]$_2$: Complex [Fe(**7**)$_2$][PF$_6$]$_2$ (54.7 mg, 0.032 mmol) was dissolved in dichloromethane (40 mL) at room temperature to obtain a 0.0008 M solution. A solution of the catalyst (Grubbs I ruthenium carbene, 2.6 mg, 10 mol%) in dichloromethane (1 mL) was then added and the mixture was stirred for 16 h at room temperature. The solvent was evaporated and the residue was purified by chromatography on Al_2O_3 by using dichloromethane/methanol (100:4) as the eluent to give catenane [Fe(**8**)][PF$_6$]$_2$ in 75% yield (39.9 mg). ^{1}H NMR ($CDCl_3$, 300 MHz): δ = 8.92 (s, 4H; H_4), 8.81 (d, 4H, J = 8.1 Hz; H_{py1}), 8.41 (t, 2H, J = 8.1 Hz; H_{py2}), 8.06 (d, 4H, J = 8.4 Hz; H_5), 7.73 (m, 4H; H_6), 7.68 (s, 4H; H_1), 7.47 (d, 4H, J = 7.2 Hz; H_7), 7.10 (d, 8H, J = 8.6 Hz; H_o), 6.79 (d, 8H, J = 8.6 Hz; H_m), 6.19 (s, 3.5H; $H_{c4\,cis}$), 6.08 (s, 0.5H; $H_{c4\,trans}$), 4.53 (m, 8H; H_{c1}), 4.38 (s, 8H; H_{c3}), 4.14 ppm (m, 8H; H_{c2}); MS (ES): m/z calcd for $C_{86}H_{74}N_6O_8Fe$: 687.245 [M/2]; found: 687.252.

[Fe(9)][PF$_6$]$_2$: Catenane [Fe(**8**)][PF$_6$]$_2$ (38.5 mg, 0.0232 mmol) was dissolved in a 1:1 mixture of CH_2Cl_2/EtOH (50 mL). The catalyst (Pd/C 10 mol%, 0.125 mg) was then added and the resulting mixture was stirred overnight under an H_2 atmosphere. The solvent was evaporated and the residue was purified by chromatography on Al_2O_3 by using dichloromethane/methanol (100:4) as the eluent. After evaporation of the solvent from the collected fractions, the solid was dissolved in dichloromethane, a saturated aqueous solution of KPF_6 (4 mL) was added, the organic solvent was evaporated and the precipitate was collected by filtration. The catenane [Fe(**9**)][PF$_6$] was obtained in almost quantitative yield (38.5 mg,

99%). ^{1}H NMR ($CDCl_3$, 300 MHz): δ = 8.94 (s, 4H; H_4), 8.81 (d, 4H, J = 8.1 Hz; H_{py1}), 8.39 (t, 2H, J = 8.1 Hz; H_{py2}), 8.04 (d, 4H, J = 8.1 Hz; H_5), 7.72 (s, 4H; H_1), 7.68 (d, 4H, J = 7.8 Hz; H_6), 7.44 (d, 4H, J = 6.6 Hz; H_7), 7.06 (d, 8H, J = 8.6 Hz; H_o), 6.75 (d, 8H, J = 8.6 Hz; H_m), 7.06 (d, 8H, J = 8.6 Hz), 4.42 (m, 8H), 4.06 (m, 8H), 3.86 (m, 8H), 1.99 ppm (m, 8H); UV/Vis (acetonitrile): λ_{max} (ε) = 542 (4670), 451 (6540), 369 (34950), 290 (30200), 248 nm (70600 $mol^{-1} dm^3 cm^{-1}$); MS (ES): m/z calcd for $C_{86}H_{70}N_6O_8Fe$: 685.230 [M/2]; found: 685.229.

[Co(7)$_2$][PF$_6$]$_3$: Compound **7** (56.2 mg, 0.082 mmol) was placed in a round-bottom flask (25 mL) and dissolved in acetonitrile (12.5 mL). A solution of $Co(NO_3)_2{\cdot}6H_2O$ (11.9 mg, 0.041 mmol) in acetonitrile (12.5 mL) was then added and the reaction was stirred at room temperature for 30 min. After this time, a solution of $[NH_4]_2[Ce(NO_3)_6]$ (22.43 mg, 0.0409 mmol) in acetonitrile (22 mL) was added dropwise to the mixture over a period of 15 min and stirring was continued for 15 min. The organic solvents were evaporated under reduced pressure, and the solid residue was dissolved in acetonitrile (35 mL). A saturated aqueous solution of KPF_6 (4 mL) was added, the organic solvent was evaporated and the precipitate was collected by filtration. The acyclic complex [Co(**7**)$_2$][PF$_6$]$_3$ was obtained as an orange solid (112 mg, 73%). ^{1}H NMR (CD_3CN, 300 MHz): δ = 8.89 (s, 4H; H_4), 8.53 (s, 6H; H_{py1}, H_{py2}), 7.92 (d, 4H, J = 8.1 Hz; H_5), 7.78 (t, 4H, J = 7.7 Hz; H_6), 7.54 (d, 4H, J = 7.2 Hz; H_7), 7.54 (s, 4H; H_1), 6.88 (d, 8H, J = 8.6 Hz; H_o), 6.74 (d, 8H, J = 8.6 Hz; H_m), 5.93 (ddt, 4H, J = 17.2, 10.2, 5.4 Hz; H_{c4}), 5.30 (d, 4H, J = 17.2 Hz; H_{c5}), 5.12 (d, 4H, J = 10.2 Hz; H_{c6}), 4.21 (m, 8H; H_{c1}), 4.06 (d, 8H, J = 5.4 Hz; H_{c3}), 3.81 ppm (m, 8H; H_{c2}); MS (ES): m/z calcd for $C_{90}H_{78}N_6O_8Co$: 476.507 [M/3], 714.760 [M/2]; found: 476.500, 714.757.

[Co(8)][PF$_6$]$_3$: A solution of the catalyst (Grubbs I ruthenium carbene, 2,8 mg, 10 mol%) in dichloromethane (1 mL) was added to a solution of complex [Co(**7**)$_2$][PF$_6$]$_3$ (62.9 mg, 0.0337 mmol) in degassed dichloromethane (40 mL). After 16 h of stirring, more of the catalyst (1.4 mg, 5 mol%) was added to the mixture as the reaction was incomplete. Another portion of the catalyst (1.4 mg, 5 mol%) was added to the mixture after 24 h of stirring for the same reason and the reaction was stirred at room temperature for another 24 h. The organic solvents were evaporated and the solid residue was dissolved in acetonitrile (35 mL). A solution of $[NH_4]_2[Ce(NO_3)_6]$ (5.4 mg, 0.0098 mmol) in acetonitrile (12 mL) was added dropwise to the mixture over a period of 15 min and stirring was continued for another 15 min. Finally, the solvent was evaporated and the residue was purified by chromatography on Al_2O_3 by using dichloromethane/acetonitrile (1:1) as the eluent. After evaporation of the collected fractions, the solid was dissolved in acetonitrile, a saturated aqueous solution of KPF_6 (4 mL) was added, the organic solvent was evaporated and the precipitate was collected by filtration. The catenane [Co(**8**)][PF$_6$]$_3$ was obtained as a yellow powder in 70% yield (42.7 mg). ^{1}H NMR (CD_3CN, 300 MHz): δ = 9.10 (s, 4H; H_4), 8.78 (d, 4H, J = 8.1 Hz; H_{py1}), 8.58 (t, 2H, J = 8.1 Hz; H_{py2}), 8.13 (d, 4H, J = 8.2 Hz; H_5), 7.99 (dd, 4H, J = 8.1, 7.2 Hz; H_6), 7.73 (d, 4H, J = 7.2 Hz; H_7), 7.62 (s, 3H; H_1), 7.59 (s, 1H; H_1), 7.09 (d, 8H, J = 8.4 Hz; H_o), 6.96 (d, 8H, J = 8.4 Hz; H_m), 6.19 (s, 3H; $H_{c4\,cis}$), 6.06 (s, 1H; $H_{c4\,trans}$), 4.42 (m, 12H; H_{c1}, H_{c3}), 4.04 ppm (m, 8H; H_{c2}); MS (ES): m/z calcd for $C_{86}H_{70}N_6O_8Co$: 457.819 [M/3], 686.729 [M/2]; found: 457.818, 686.725.

[Co(9)][PF$_6$]$_3$: Complex [Co(**8**)][PF$_6$] (40 mg, 0.0221 mmol) was dissolved in a mixture of CH_2Cl_2 (16 mL) and EtOH (4 mL). The catalyst (Pd/C, 24.6 mg, 0,0221 mmol) was then added and the resulting mixture was stirred at room temperature for 36 h under an H_2 atmosphere. After filtration through Celite, the solvents were evaporated. TLC on alumina eluted with dichloromethane/acetonitrile (3:2) revealed the presence of cobalt(II) complexes. The compound was dissolved in acetonitrile (12 mL) and oxidised by addition of a solution of $[NH_4]_2[Ce(NO_3)_6]$ (4.8 mg, mmol) in a mixture of acetonitrile (10 mL) and dichloromethane (6 mL) over a period of 15 min. Stirring was continued for a further 15 min. After evaporation of the solvents, the residue was purified by chromatography on Al_2O_3 by using dichloromethane/acetonitrile (1:1) as the eluent. After evaporation of the solvent from the collected fractions, the solid was dissolved in dichloromethane, a saturated aqueous solution of KPF_6 (4 mL) was added, the organic solvent was evaporated and the precipitate was collected by filtration. The final catenane [Co(**9**)][PF$_6$]$_3$ was obtained as a yellow powder in 60% yield (24 mg). ^{1}H NMR ($CDCl_3$, 300 MHz): δ = 9.12 (s, 4H; H_4), 8.78 (d, 4H, J = 7.8 Hz; H_{py1}), 8.64 (t, 2H, J = 7.8 Hz; H_{py2}), 8.13 (d, 4H, J = 8.4 Hz; H_5), 7.99 (dd, 4H, J = 7.5, 7.8 Hz; H_6), 7.73 (d, 4H, J = 7.0 Hz; H_7), 7.64 (s, 4H; H_1), 7.09 (d, 8H, J = 8.6 Hz; H_o), 6.97 (d, 8H, J = 8.6 Hz; H_m), 4.34 (m, 8H; H_{c1}), 3.98 (m, 8H; H_{c2}), 3.83 (m, 8H; H_{c3}), 1.96 ppm (m, 8H; H_{c4}); UV/Vis (acetonitrile): λ_{max} (ε) = 400 (shoulder), 374 (39450), 247 nm (132400 $mol^{-1} dm^3 cm^{-1}$); MS (ES): m/z calcd for $C_{86}H_{74}N_6O_8Co$: 459.163 [M/3], 688.744 [M/2]; found: 459.151, 688.721.

Acknowledgements

We are grateful to the CNRS and the Région Alsace for fellowships to J. Lux.

[1] For review articles and books on catenanes and rotaxanes, see references [2–9].
[2] G. Schill, *Catenanes, Rotaxanes and Knots: Organic Chemistry Monographs*, Academic Press, New York, **1971**, p. 22.
[3] C. O. Dietrich-Buchecker, J.-P. Sauvage, *Chem. Rev.* **1987**, *87*, 795–810.
[4] D. B. Amabilino, J. F. Stoddart, *Chem. Rev.* **1995**, *95*, 2725–2828.
[5] F. Vögtle, T. Dünnwald, T. Schmidt, *Acc. Chem. Res.* **1996**, *29*, 451–460.
[6] *Catenanes, Rotaxanes and Knots. A Journey Through the World of Molecular Topology* (Eds.: C. Dietrich-Buchecker, J.-P. Sauvage), Wiley-VCH, Weinheim, **1999**.
[7] M. Fujita, *Acc. Chem. Res.* **1999**, *32*, 53–61.
[8] A. Harada, *Acc. Chem. Res.* **2001**, *34*, 456–464.
[9] P. D. Beer, M. R. Sambrook, D. Curiel, *Chem. Commun.* **2006**, 2105–2117.
[10] a) C. O. Dietrich-Buchecker, J.-P. Sauvage, J.-P. Kintzinger, *Tetrahedron Lett.* **1983**, *24*, 5095–5098; b) C. O. Dietrich-Buchecker, J.-P. Sauvage, J.-M. Kern, *J. Am. Chem. Soc.* **1984**, *106*, 3043–3045; c) A. M. Albrecht-Gary, Z. Saad, C. O. Dietrich-Buchecker, J.-P. Sauvage, *J. Am. Chem. Soc.* **1985**, *107*, 3205–3209.
[11] a) J.-M. Kern, J.-P. Sauvage, G. Bidan, M. Billon, B. Divisia-Blohorn, *Adv. Mater.* **1996**, *8*, 580–582; b) M. Billon, B. Divisia-Blohorn, J.-M. Kern, J.-P. Sauvage, *J. Mater. Chem.* **1997**, *7*, 1169–1173.
[12] J.-C. Chambron, C. O. Dietrich-Buchecker, J.-P. Sauvage in *Comprehensive Supramolecular Chemistry, Vol. 9* (Eds.: J. L. Atwood, J. E. D. Davies, D. D. MacNicol, F. Vögtle, J.-M. Lehn, J.-P. Sauvage, M. W. Hosseini), Pergamon, Oxford, **1999**, pp. 43–83.
[13] B. Mohr, M. Weck, J.-P. Sauvage, *Angew. Chem.* **1997**, *109*, 1365–1367; *Angew. Chem. Int. Ed. Engl.* **1997**, *36*, 1308–1310.
[14] a) G. Rapenne, C. O. Dietrich-Buchecker, J.-P. Sauvage, *J. Am. Chem. Soc.* **1999**, *121*, 994–1001; b) C. O. Dietrich-Buchecker, J.-P. Sauvage, *Chem. Commun.* **1999**, 615–616.
[15] a) C. Hamann, J. M. Kern, J. P. Sauvage, *Dalton Trans.* **2003**, 3770–3775; b) C. Hamann, J.-M. Kern, J.-P. Sauvage, *Inorg. Chem.* **2003**, *42*, 1877–1883; c) J.-P. Collin, C. Dietrich-Buchecker, C. Hamann, D. Jouvenot, J.-M. Kern, P. Mobian, J.-P. Sauvage in *Comprehensive Coordination Chemistry II, Vol. 7* (Eds.: J. A. McCleverty, T. J. Meyer), **2004**, pp. 303–326.
[16] J.-C. Chambron, J.-P. Collin, V. Heitz, D. Jouvenot, J.-M. Kern, P. Mobian, D. Pomeranc, J.-P. Sauvage, *Eur. J. Org. Chem.* **2004**, 1627–1638.
[17] C. O. Dietrich-Buchecker, B. X. Colasson, J.-P. Sauvage, *Top. Curr. Chem.* **2005**, *249*, 261–284.
[18] a) C. Wu, P. R. Lecavalier, Y. X. Shen, H. W. Gibson, *Chem. Mater.* **1991**, *3*, 569–572; b) J. D. Megiatto, Jr., D. I. Schuster, *Org. Lett.* **2011**, *13*, 1808–1811, and references therein.
[19] a) D. A. Leigh, P. J. Lusby, S. J. Teat, A. J. Wilson, J. K. Y. Wong, *Angew. Chem.* **2001**, *113*, 1586–1591; *Angew. Chem. Int. Ed.* **2001**, *40*, 1538–1543; b) D. A. Leigh, P. J. Lusby, R. T. McBurney, A. Mor-

elli, A. M. Z. Slawin, A. R. Thomson, D. B. Walker, *J. Am. Chem. Soc.* **2009**, *131*, 3762–3771.
[20] a) M. Fujita, F. Ibukuro, H. Hagihara, K. Ogura, *Nature* **1994**, *367*, 720; b) M. Fujita, M. Aoyagi, F. Ibukuro, K. Ogura, K. Yamaguchi, *J. Am. Chem. Soc.* **1998**, *120*, 611–612.
[21] S. S. Zhu, P. J. Carroll, T. M. Swager, *J. Am. Chem. Soc.* **1996**, *118*, 8713–8714.
[22] A. M. Fuller, D. A. Leigh, P. J. Lusby, I. D. H. Oswald, S. Parsons, D. B. Walker, *Angew. Chem.* **2004**, *116*, 4004–4008; *Angew. Chem. Int. Ed.* **2004**, *43*, 3914–3918.
[23] Y. Furusho, T. Matsuyama, T. Takata, T. Moriuchi, T. Hirao, *Tetrahedron Lett.* **2004**, *45*, 9593–9597.
[24] a) A. M. L. Fuller, D. A. Leigh, P. J. Lusby, A. M. Z. Slawin, D. B. Walker, *J. Am. Chem. Soc.* **2005**, *127*, 12612–12619; b) S. M. Goldup, D. A. Leigh, P. J. Lusby, R. T. McBurney, A. M. Z. Slawin, *Angew. Chem.* **2008**, *120*, 7107–7111; *Angew. Chem. Int. Ed.* **2008**, *47*, 6999–7003; c) J. E. Beves, B. A. Blight, C. J. Campbell, D. A. Leigh, R. T. McBurney, *Angew. Chem.* **2011**, *123*, 9428–9499; *Angew. Chem. Int. Ed.* **2011**, *50*, 9260–9327.
[25] a) S. J. Cantrill, K. S. Chichak, A. J. Peters, J. F. Stoddart, *Acc. Chem. Res.* **2005**, *38*, 1–9; b) F. Aricó, J. D. Badjic, S. J. Cantrill, A. H. Flood, K. C.-F. Leung, Y. Liu, J. F. Stoddart, *Top. Curr. Chem.* **2005**, *249*, 203–259.
[26] a) J.-P. Sauvage, M. Ward, *Inorg. Chem.* **1991**, *30*, 3869–3874; b) N. Belfrekh, C. Dietrich-Buchecker, J.-P. Sauvage, *Inorg. Chem.* **2000**, *39*, 5169–5172.
[27] a) D. Pomeranc, D. Jouvenot, J.-C. Chambron, J.-P. Collin, V. Heitz, J.-P. Sauvage, *Chem. Eur. J.* **2003**, *9*, 4247–4254; b) P. Mobian, J.-M. Kern, J.-P. Sauvage, *J. Am. Chem. Soc.* **2003**, *125*, 2016–2017; c) J.-P. Collin, D. Jouvenot, M. Koizumi, J.-P. Sauvage, *Eur. J. Inorg. Chem.* **2005**, 1850–1855.
[28] a) A. I. Prikhod'ko, F. Durola, J.-P. Sauvage, *J. Am. Chem. Soc.* **2008**, *130*, 448–449; b) A. I. Prikhod'ko, J.-P. Sauvage, *J. Am. Chem. Soc.* **2009**, *131*, 6794–6807.
[29] J. C. Loren, P. Gantzel, A. Linden, J. S. Siegel, *Org. Biomol. Chem.* **2005**, *3*, 3105–3116.
[30] K. S. Chichak, S. J. Cantrill, A. R. Pease, S.-H. Chiu, G. W. V. Cave, J. L. Atwood, J. F. Stoddart, *Science* **2004**, *304*, 1308–1312.
[31] CuAAC active-metal template: a) V. Aucagne, K. D. Hänni, D. A. Leigh, P. J. Lusby, D. B. Walker, *J. Am. Chem. Soc.* **2006**, *128*, 2186–2187; b) V. Aucagne, J. Berná, J. D. Crowley, S. M. Goldup, K. D. Hänni, D. A. Leigh, P. J. Lusby, V. E. Ronaldson, A. M. Z. Slawin, A. Viterisi, D. B. Walker, *J. Am. Chem. Soc.* **2007**, *129*, 11950–11963; c) S. M. Goldup, D. A. Leigh, T. Long, P. R. McGonigal, M. D. Symes, J. Wu, *J. Am. Chem. Soc.* **2009**, *131*, 15924–15929; d) S. M. Goldup, D. A. Leigh, P. R. McGonigal, V. E. Ronaldson, A. M. Z. Slawin, *J. Am. Chem. Soc.* **2010**, *132*, 315–320; e) H. Lahlali, K. Jobe, M. Watkinson, S. M. Goldup, *Angew. Chem.* **2011**, *123*, 4237–4241; *Angew. Chem. Int. Ed.* **2011**, *50*, 4151–4155.
[32] Glaser and Ullman active-metal template: a) S. Saito, E. Takahashi, K. Nakazono, *Org. Lett.* **2006**, *8*, 5133–5136; b) Y. Sato, R. Yamasaki, S. Saito, *Angew. Chem.* **2009**, *121*, 512–515; *Angew. Chem. Int. Ed.* **2009**, *48*, 504–507.
[33] Pd^{II}-catalysed Michael addition: S. M. Goldup, D. A. Leigh, P. J. Lusby, R. T. McBurney, A. M. Z. Slawin, *Angew. Chem.* **2008**, *120*, 3429–3432; *Angew. Chem. Int. Ed.* **2008**, *47*, 3381–3384.
[34] Heck cross-coupling: a) J. D. Crowley, K. D. Hänni, A.-L. Lee, D. A. Leigh, *J. Am. Chem. Soc.* **2007**, *129*, 12092–12093; b) J. Berná, J. D. Crowley, S. M. Goldup, K. D. Hänni, A.-L. Lee, D. A. Leigh, *Angew. Chem.* **2007**, *119*, 5811–5815; *Angew. Chem. Int. Ed.* **2007**, *46*, 5709–5713; c) T. M. Swager, R. M. Moslin, *Synfacts* **2007**, 1158; d) J. Berná, S. M. Goldup, A.-L. Lee, D. A. Leigh, M. D. Symes, G. Teobaldi, F. Zerbetto, *Angew. Chem.* **2008**, *120*, 4464–4468; *Angew. Chem. Int. Ed.* **2008**, *47*, 4392–4396; e) see also, reference [19c].
[35] Nickel-catalysed homocoupling: S. M. Goldup, D. A. Leigh, R. T. McBurney, P. R. McGonigal, A. Plant, *Chem. Sci.* **2010**, *1*, 383–386.
[36] Nickel–Copper-catalysed homocoupling: J. D. Crowley, S. M. Goldup, N. D. Gowans, D. A. Leigh, V. E. Ronaldson, A. M. Z. Slawin, *J. Am. Chem. Soc.* **2010**, *132*, 6243–6248.
[37] Cu^{I} catalysed Diels–Alder: J. D. Crowley, K. D. Hänni, D. A. Leigh, A. M. Z. Slawin, *J. Am. Chem. Soc.* **2010**, *132*, 5309–5314.
[38] a) J. D. Crowley, S. M. Goldup, A. L. Lee, D. A. Leigh, R. T. McBurney, *Chem. Soc. Rev.* **2009**, *38*, 1530–1541; b) see also, reference [24d].
[39] a) F. Durola, J.-P. Sauvage, O. S. Wenger, *Chem. Commun.* **2006**, 171–173; b) F. Durola, L. Russo, J.-P. Sauvage, K. Rissanen, O. S. Wenger, *Chem. Eur. J.* **2007**, *13*, 8749–8753; c) F. Durola, D. Hanss, P. Roesel, J.-P. Sauvage, O. S. Wenger, *Eur. J. Org. Chem.* **2007**, 125–135; d) F. Durola, J.-P. Sauvage, O. S. Wenger, *Helv. Chim. Acta* **2007**, *90*, 1439–1446.
[40] a) P. Marnot, PhD Thesis, Université de Strasbourg (France), **1984**; b) C. O. Dietrich-Buchecker, P. A. Marnot, J.-P. Sauvage, J.-P. Kintzinger, P. Maltese, *Nouv. J. Chim.* **1984**, *8*, 573–582.
[41] J. R. Kirchhoff, D. R. McMillin, P. A. Marnot, J.-P. Sauvage, *J. Am. Chem. Soc.* **1985**, *107*, 1138–1141.
[42] a) P. Schwab, R. H. Grubbs, J. W. Ziller, *J. Am. Chem. Soc.* **1996**, *118*, 100–110; b) T. M. Trnka, R. H. Grubbs, *Acc. Chem. Res.* **2001**, *34*, 18–29.
[43] V. Goral, M. I. Nelen, A. V. Eliseev, J.-M. Lehn, *Proc. Natl. Acad. Sci. USA* **2001**, *98*, 1347–1352.
[44] J. Chambers, B. Eaves, D. Parker, R. Claxton, P. S. Ray, S. J. Slattery, *Inorg. Chim. Acta* **2006**, *359*, 2400–2406.
[45] A. R. Guadalupe, D. A. Usifer, K. T. Potts, H. C. Humell, A.-E. Mogstad, H. D. Abruna, *J. Am. Chem. Soc.* **1988**, *110*, 3462–3466.
[46] S. H. Wadman, M. Lutz, D. M. Tooke, A. L. Spek, F. Hartl, R. W. A. Havenith, G. P. M. van Klink, G. van Koten, *Inorg. Chem.* **2009**, *48*, 1887–1900.
[47] F. Barigelletti, B. Ventura, J.-P. Collin, R. Kayhanian, P. Gaviña, J.-P. Sauvage, *Eur. J. Inorg. Chem.* **2000**, 113–119.
[48] E. C. Constable, G. Baum, E. Bill, R. Dyson, R. van Eldik, D. Fenske, S. Kaderli, D. Morris, A. Neubrand, M. Neuburger, D. R. Smith, K. Wieghardt, M. Zehnder, A. D. Zuberbuhler, *Chem. Eur. J.* **1999**, *5*, 498–508.
[49] V. Balzani, G. Bergamini, S. Campagna, F. Puntoriero, *Top. Curr. Chem.* **2007**, *280*, 1–36.
[50] B. Ventura, F. Barigelletti, F. Durola, L. Flamigni, J.-P. Sauvage, O. S. Wenger, *Dalton Trans.* **2008**, 491–498.
[51] P. S. Braterman, J. I. Song, R. D. Peacock, *Inorg. Chem.* **1992**, *31*, 555–559.
[52] R. A. Palmer, T. S. Piper, *Inorg. Chem.* **1966**, *5*, 864–878.
[53] *Kappa CCD Operation Manual*, Nonius, Delft, **1997**.
[54] SHELXS-97 Program for Crystal Structure Determination: G. M. Sheldrick, *Acta Crystallogr. A* **1990**, *46*, 467–473.
[55] G. Sheldrick, *SHELXL-97*, Universität Göttingen, Göttingen, **1999**.
[56] A. L. Spek, *J. Appl.Cryst.* **2003**, *36*, 7–13.
[57] *M86-E01078 APEX2 User Manual*, Bruker AXS Inc., Madison, **2006**.

Received: December 28, 2011
Published online: March 19, 2012

